Sains Malaysiana 42(8)(2013): 1151–1157

# Optical Properties of Poly(9,9'-di-n-octylfluorenyl-2.7-diyl)/Amorphous $SiO_2$ Nanocomposite Thin Films

(Sifat Optik Filem Nipis Nanokomposit Poli(9,9'-di-n-ostilfluorenyl-2.7-diil)/Amorfus $SiO_2$)

MOHAMMAD HAFIZUDDIN HAJI JUMALI*, BANDAR ALI AL-ASBAHI, CHI CHIN YAP, MUHAMAD MAT SALLEH & MOHAMAD SALEH ALSALHI

ABSTRACT

*Identified as potential materials for optoelectronic applications, the polymer/inorganic nanocomposites are actively studied. In this work, the effect of amorphous silica nanoparticles (NPs) content on the optical properties of Poly (9,9'-di-n-octylfluorenyl- 2.7-diyl) (PFO) thin films has been investigated. Different ratios of PFO/$SiO_2$ NPs composites have been prepared using solution blending method. Then, the blends were spin-coated onto glass substrates at 2000 rpm for 30 s and subsequently dried at room temperature. XRD and TEM were used to determine the structural properties, while UV-Vis and PL spectrophotometers were employed to investigate the optical properties of the films. XRD confirms that there was no variation on structure of both PFO and $SiO_2$ NPs resulted from the blending process. TEM micrographs display that majority of amorphous $SiO_2$ NPs were well coated with PFO. The absorption spectra of the composite thin films were red-shifted, indicating the increment in conjugation length of the PFO/$SiO_2$ composite. In addition, the calculated values of the optical energy gap, the width of the energy tails and vibronic spacing of the composite films exhibited $SiO_2$ content dependence.*

*Keywords: Absorption; energy gap; energy tail; photoluminescence; vibronic spacing*

ABSTRAK

*Dikenal pasti sebagai bahan berpotensi untuk kegunaan optoelektronik, nanokomposit polimer/bahan inorganik sedang dikaji secara aktif. Dalam kajian ini kesan kandungan nanozarah amorfus $SiO_2$ ke atas sifat optik filem nipis poli(9,9'-di-n-ostilfluorenyl-2.7-diil) (PFO) telah dikaji. Larutan PFO/$SiO_2$ yang berbeza nisbah telah disediakan menggunakan teknik adunan larutan. Kemudian, adunan dimendapkan ke atas substrat kaca menggunakan teknik salutan berputar pada kelajuan 2000 ppm selama 30 s dan seterusnya dikeringkan pada suhu bilik selama 1 jam. XRD dan TEM digunakan untuk pencirian struktur sementara spektrofotometer UV-Vis dan PL digunakan untuk mengkaji sifat optik filem yang disediakan. Pencirian XRD tidak menunjukkan sebarang perubahan struktur ke atas PFO dan nanozarah $SiO_2$ akibat dari proses adunan. Mikrograf TEM menunjukkan nanozarah amorfus $SiO_2$ tersalut oleh PFO. Berbanding spektrum penyerapan filem PFO, spektrum penyerapan untuk filem nipis nanokomposit mempamerkan anjakan merah, menandakan pertambahan panjang konjugasi PFO/$SiO_2$. Selain itu, nilai bagi jurang tenaga, lebar ekor tenaga dan jarak vibronik oleh filem komposit juga menunjukkan pergantungan kepada kandungan $SiO_2$.*

*Kata kunci: Ekor tenaga; fotoluminesen; jarak vibronik; jurang tenaga; penyerapan*

## INTRODUCTION

Polymer/inorganic nanocomposites have been identified as the potential materials for many applications such as light-emitting diodes (LEDs), solar cells and sensors. This is due to their excellent properties arising from the synergic reaction between the properties of these two different materials. Despite earlier setbacks (Carter et al. 1997; Ho & Friend 2002), more recent studies proved otherwise. The formation of homogeneous nanocomposites successfully improved physicochemical stability and conductivity of the polymer host (Huang et al. 2010; Kickelbick 2003; Kim & Park 2012; Peng et al. 2005; Uragami et al. 2005).

One of the major advantages of hybridization is the creation of unique optical properties of the hybrid materials. As example, poly(phenylene vinylene)s (PPV)/$SiO_2$ nanocomposites exhibited blue shift in photoluminescence emission, indicating a reduction in the conjugation lengths of polymer matrix (Yang et al. 2005). More importantly, additions of inorganic material were reported to enhance luminescent stability (Yang et al. 2007), reduce the optical energy gap (Ibrahim et al. 2012) and provide greater control on the emission band width (Liu et al. 2001). The improvement in optical properties of these hybrid materials has been explained in detail (Tommalieh & Zihlif 2010).

Despite these great achievements, there are limited reports on the more fundamental optoelectronic properties of nanocomposites. Alongside energy gaps, determination of other parameters such as energy tails and vibronic

spacing is crucial especially for predicting the performance of optoelectronic devices.

It is well known that the energy gap of $SiO_2$ NPs is 9 eV (Dutta & De 2006) while PFO has energy gap of ~ 3eV (Bajpai et al. 2010). Since the energy gap differs significantly, the lowest unoccupied molecular orbital (LUMO) of PFO is lower than conduction band of $SiO_2$ and highest occupied molecular orbital (HOMO) of PFO is higher than valence band of $SiO_2$ (Liu et al. 2007). With such energy bands structures, the charge trapping which is crucial for improved performance of optoelectronic devices (reduce turn on voltage, enhance luminance and luminence efficiency) is expected to be effective in the PFO/$SiO_2$ nanocomposite. Unlike energy gap, all these parameters are indirectly depended upon the creation of delocalized state in the forbidden gap of the materials' band structures. The creation of delocalized state is indicated directly by increase in the width of the energy tails and indirectly by reduction in vibronic spacing.

In this work we report on the fundamental optoelectronic properties of PFO/$SiO_2$ amorphous nanoparticles composites thin films. As a derivative of polyfluorene, PFO exhibits better photo- and thermal-stability than the commonly used PPV (Assaka et al. 2004). The optoelectronic properties of this nanocomposites thin films namely energy gaps (direct and indirect), width of the energy tails and vibronic spacing energy were calculated. In addition, the effect of nanoparticles contents on these properties was also discussed.

## Experimental Details

$SiO_2$ nanoparticles (NPs) were synthesized based on the earlier published work (Jafarzadeh et al. 2009). Initially 5 mL of tetraethyl orthosilicate (TEOS, 99%, Fluka) was completely dissolved in 30 mL of absolute ethanol at room temperature for 10 min. Then, 1 mL of distilled water was dropped at a rate of 0.2 mL $min^{-1}$ into the reaction media to facilitate the hydrolysis of TEOS in the ultrasonic bath. After 1 h, 2 mL of ammonia ($NH_3$, 25%, Fluka) was added into the reaction mixture at a rate of 0.01 mL $min^{-1}$. Sonication was continued for another 3 h to get a white turbid suspension followed by gelation process for 1 h. Finally, the gel was centrifuged and washed with ethanol and distilled water and subsequently heated at intermediate temperature for removal of the remaining organic element. Commercial PFO (Sigma Aldrich with average $M_w$ of 58.200) has been used in this study. To prepare the PFO/$SiO_2$ nanocomposites, appropriate amount of PFO was dissolved in tetrahydrofuran (THF) to form PFO solution with concentration of 3 mg/mL. Next, different weight ratios of $SiO_2$ NPs (10-70 wt.%) were added into the solution. The solutions were stirred at 600 rpm overnight, followed by sonication for 1 h to yield homogeneous nanocomposites. Then, 70 µL solution was deposited onto a glass substrate (1.2 cm × 2 cm) using spin coating technique (rotational speed of 2000 rpm for 30 s). Finally, it was left to dry at room temperature.

The structural characterization was carried out using a Bruker D8 Advance X-ray Diffractometer with Cu $K_\alpha$ radiation source (l=1.5418 ) and 2θ scan angle of 20-60°. The nanostructure of the films was observed using a TEM (model Philips CM12, accelerating voltage of 100 kV). The absorption and photoluminescence (PL) spectra of the nanocomposite thin films were investigated using Perkin Elmer LAMBDA 900 UV Vis Spectrophotometer and Perkin Elmer LS55 Luminescence Spectrometer (excitation wavelength of 355 nm), respectively. The thicknesses of the films were measured using Dektak 150 surface profiler. Finally, the peaks profiles from PL curves were fitted with Gaussian function using Origin (version 7.5) software.

## Results and Discussion

The X-ray patterns for the PFO and $SiO_2$ NPs confirm that these materials were in the amorphous state and thus the PFO/$SiO_2$ nanocomposites also exhibited typical amorphous nature (Figure 1). Figure 2 displays the morphology of $SiO_2$ NPs and PFO/$SiO_2$ NPs composites. The $SiO_2$ existed as amorphous spherical particles with an average diameter of about 26.4 nm with standard deviation of 3.5 nm (Figure 2(a)). As for the composite materials, the micrograph confirms that $SiO_2$ NPs were well coated with PFO (Figure 2(b)).

The UV–Vis spectrum of PFO film (Figure 3) displays a $\lambda_{max}$ at 404 nm which corresponds to a $\Pi$–$\Pi^*$ transition (Han et al. 2010) and a shoulder around 435 nm. The absorbance wavelength was slightly red-shifted upon additions of $SiO_2$ NPs, indicating minor expansions in conjugation length. In addition, the absence of additional absorption peak in the spectra illustrates the nonexistence of interaction between PFO and $SiO_2$ at the ground states (Ginger & Greenham 1999).

The absorption coefficient was determined from the spectra using the formula (Al-Ani et al. 1999):

$$\alpha = \frac{2.303A}{d}, \quad (1)$$

where $A$ is the absorbance and $d$ is the sample thickness (Table 1). By substituting α into Tauc equation (Elliott 1998), the $(\alpha h\upsilon)^n$ versus photon energy curves were plotted. The energy band gaps for the thin films were obtained by extrapolating the linear part from the slope of the curve as shown in Figure 4. The values for $n$ are 2 and ½ for direct and indirect energy gaps, respectively. The calculated values for direct energy gaps ($E_{gd}$) and indirect energy gaps ($E_{gi}$) are presented in Table 1. It was observed that the $E_{gd}$ values decreased systematically from 2.91 to 2.76 eV upon addition of $SiO_2$ NPs, while $E_{gi}$ values dramatically reduced from 2.69 to 2.20 eV.

The absorption tails in amorphous and semi-crystalline materials could be interpreted in terms of the Dow-Redfield effect (Dow & Redfield 1970) by taking the form of Urbach rule (Urbach 1953) as follows:

$$ln(\alpha) = ln(\alpha_0) + (h\nu / \Delta E), \quad (2)$$

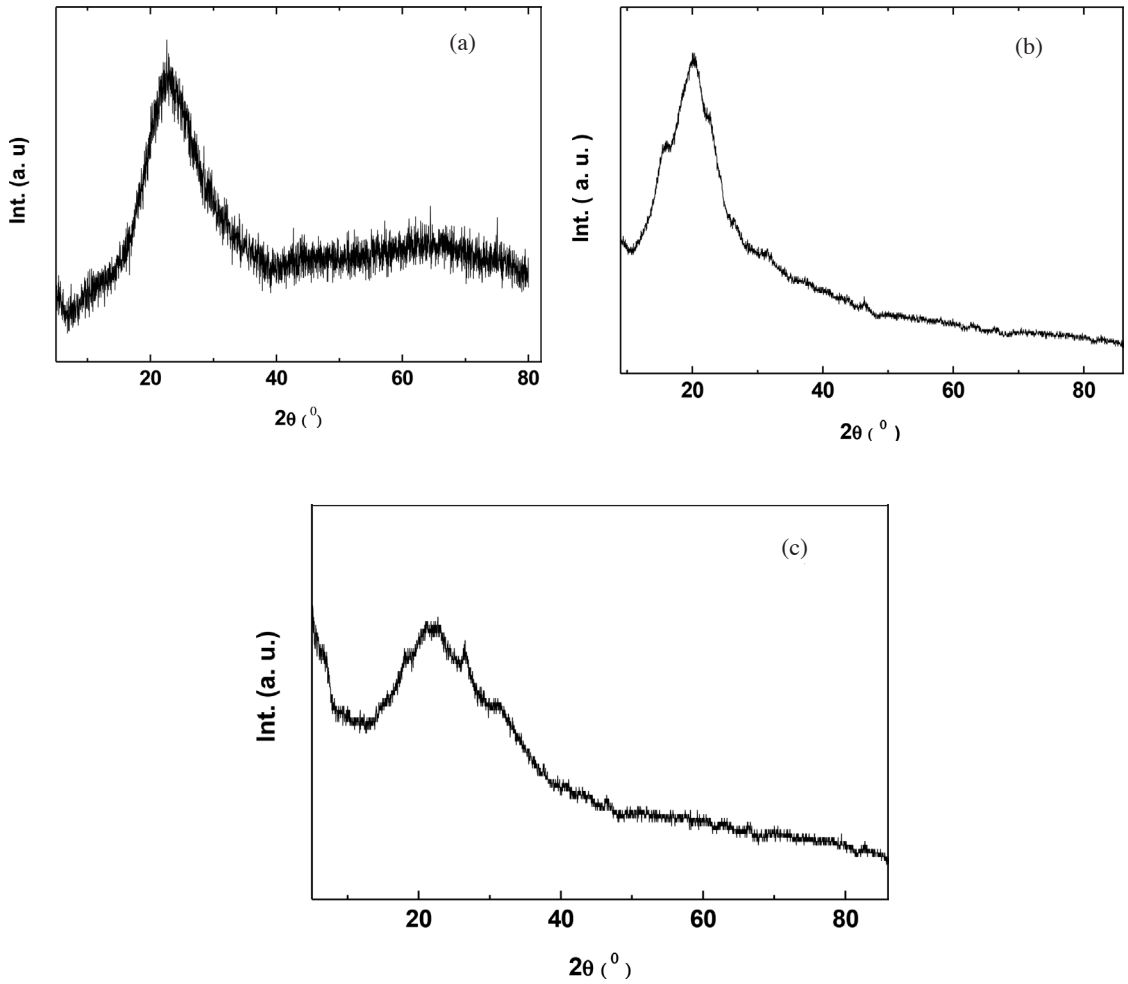


FIGURE 1. Typical XRD patterns for (a) $SiO_2$ NPs, (b) Pure PFO and (c) PFO/50 wt.% $SiO_2$ NPs

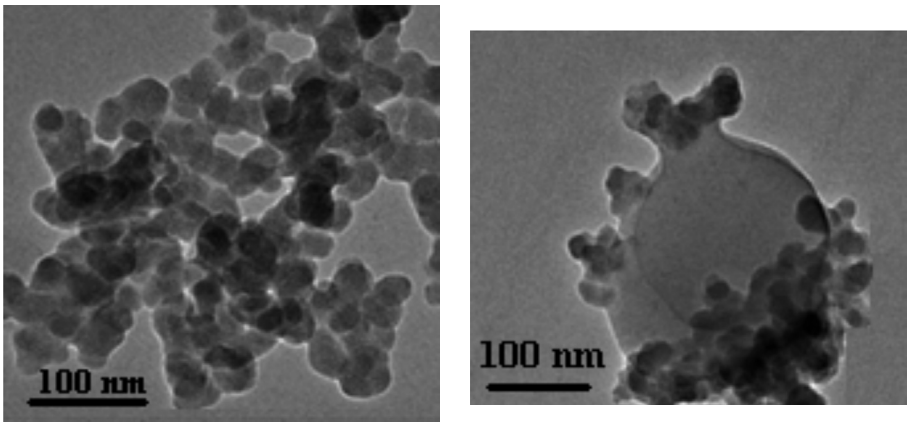


(a) (b)

FIGURE 2. TEM images of (a) $SiO_2$ NPs (b) PFO/$SiO_2$ nanocomposite (50 wt. % $SiO_2$)

where $\alpha_o$ is a constant and $\Delta E$ is the width of the energy tail which reflects the width of the tail of localized states in the forbidden band gap (Elliott 1998). Figure 5 displays the Urbach plots for the composite samples. The $\Delta E$ values were calculated from the slope of the linear part in the exponential region (region 1) of each curve (Raja et al. 2003; Tommalieh & Zihlif 2010) and listed in Table 1. Wider energy tails illustrate the creation of disorder and imperfections in the band structure of the nanocomposites (Tommalieh & Zihlif 2010) resulted from the inclusion of $SiO_2$ NPs. This observation also indicates that more localized states within the forbidden gap were created

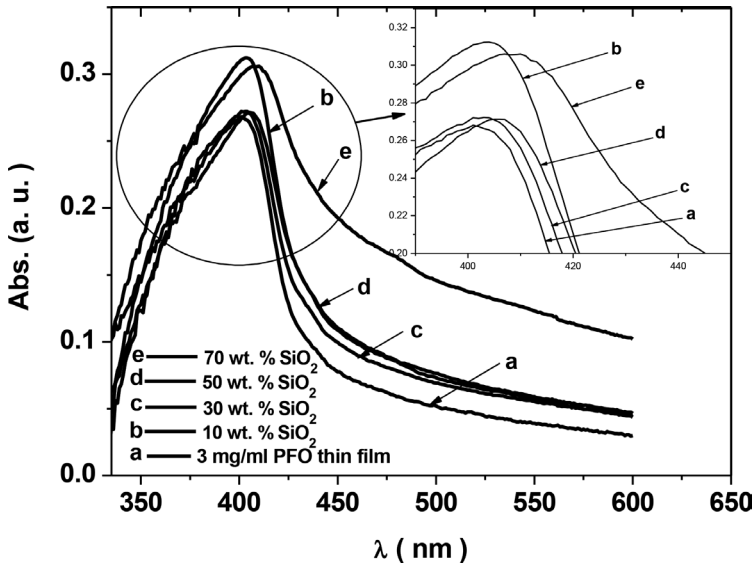


FIGURE 3. Absorption spectra for PFO and PFO/$SiO_2$ nanocomposites

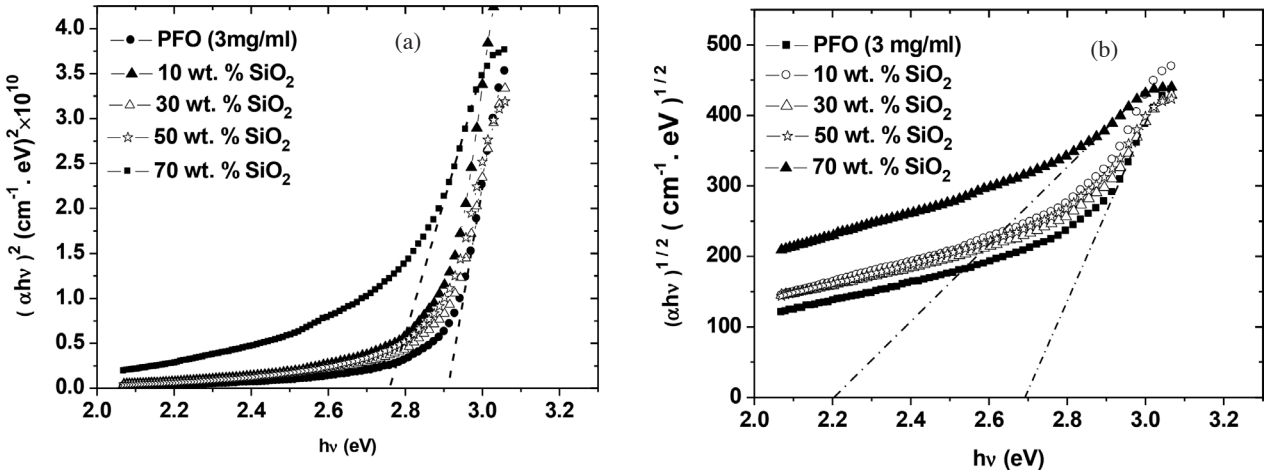


FIGURE 4. Dependence of (a): $(\alpha h\nu)^2$ and (b): $(\alpha h\nu)^{1/2}$ on photon energy ($h\nu$) for Pure PFO and PFO/$SiO_2$ nanocomposites

(Hagler et al. 1991; Pichler et al. 1993). As comparison, the width of the energy tail in PFO was lower, a direct consequence of neat polymer structure and thus greater energy gap (Tommalieh & Zihlif 2010).

PL emission spectra for all samples are shown in Figure 6. Three main emission peaks for PFO located at 427.0 nm, 442.5 nm and 467.6 nm were observed, referring to 0-0, 0-1 and 0-2 transitions, respectively. The intensities of 0-0 vibronic bands exhibited faster increment than that of 0-1 transitions up to 30 wt.% $SiO_2$ NPs before recorded lower intensity at 50 and 70 wt.%. The quenching in the intensity at higher wt% is primarily due to aggregation of inorganic NPs (Rozenberg & Tenne 2008). In addition, the 0-0 bands were red shifted upon addition of $SiO_2$ NPs; whereas the 0-1 bands were slightly blue shifted. This observation is commonly associated with increment in the conjugation length of PFO (Yang et al. 2007) which is also in a good agreement with UV-Vis observation.

By using Gaussion function, the PL curves presented in Figure 6 can be deconvoluted into four vibronic bands. The increase of $SiO_2$ weight fraction in starting charge systematically reduced the vibronic spacing energy from 0.102 to 0.076 eV (Table 1), which is commonly associated with the higher degree in chain disorder (Pichler et al. 1993).

## CONCLUSION

This work demonstrated that the optical properties of PFO thin film can be modified by controlling the amount of amorphous $SiO_2$ NPs. The absorption and emission characteristics confirm that addition of $SiO_2$ NPs remarkably influenced the optical properties and conjugated length of PFO. The decrease of both energy gap and vibronic spacing energy and increase of the energy tail upon increment of $SiO_2$ NPs, illustrate the creation of more localized states

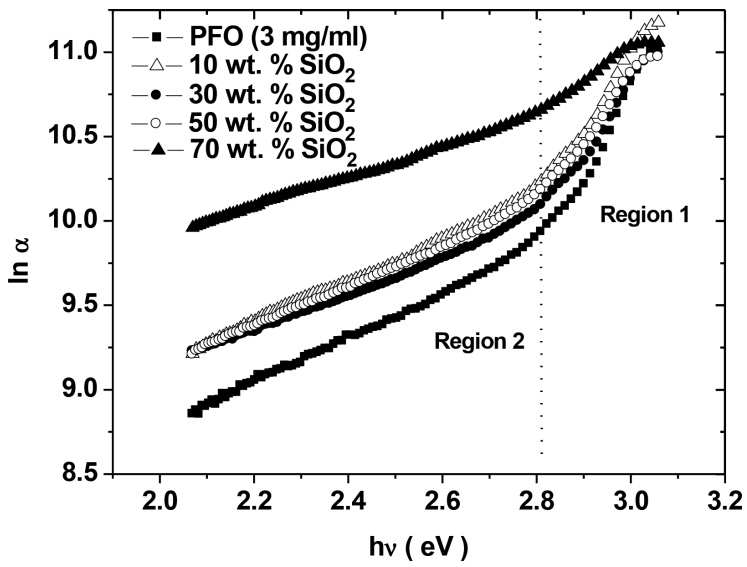


FIGURE 5. ln α as a function of photon energy for PFO and PFO/$SiO_2$ nanocomposites

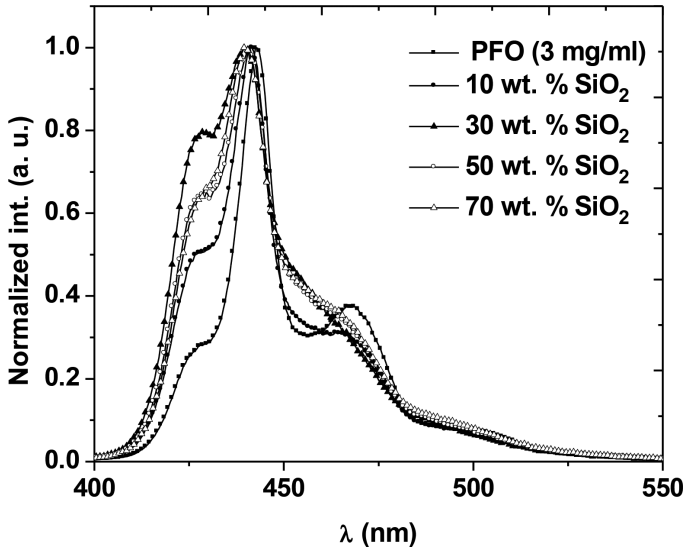


FIGURE 6. Normalized fluorescence intensity of pure PFO and PFO/$SiO_2$ nanocomposite

TABLE 1. Optical parameters of PFO and PFO/$SiO_2$ nanocomposites

| Specimens | Thickness (nm) | $E_{gd}$ (eV) | $E_{gi}$ (eV) | ΔE (eV) | Vibronic spacing (eV) |
|---|---|---|---|---|---|
| Pure PFO | 98 | 2.91 | 2.69 | 0.143 | 0.102 |
| 10% $SiO_2$ | 100 | 2.89 | 2.61 | 0.183 | 0.096 |
| 30% $SiO_2$ | 104 | 2.88 | 2.59 | 0.189 | 0.083 |
| 50% $SiO_2$ | 107 | 2.86 | 2.55 | 0.202 | 0.086 |
| 70% $SiO_2$ | 111 | 2.76 | 2.20 | 0.432 | 0.076 |

within the forbidden gap as well as higher degree of chain disorder. The fundamental information obtained from this work can be used as important tools for prediction on the suitability of these nanocomposites as active material in the optoelectronic devices.

ACKNOWLEDGEMENTS

The authors would like to thank Universiti Kebangsaan Malaysia (UKM) for providing the financial support through UKM-OUP-FST-2012 research university grant. One of the authors (Bandar Al-Asbahi) is grateful to Sana'a University, Yemen, for the PhD scholarship.

REFERENCES

Al-Ani, S.K.J., Al-Ramadin, Y., Ahmad, M.S., Zihlif, A.M., Volpe, M., Malineonico, M., Martuscelli, E. & Ragosta, G. 1999. The optical properties of polymethylmethacrylate polymer dispersed liquid crystals. *Polymer Testing* 18(8): 611-619.

Assaka, A.M., Rodrigues, P.C., De Oliveira, A.R.M., Ding, L., Hu, B., Karasz, F.E. & Akcelrud, L. 2004. Novel fluorine containing polyfluorenes with efficient blue electroluminescence. *Polymer* 45(21): 7071-7081.

Bajpai, M., Srivastava, R., Kamalasanan, M.N., Tiwari, R.S. & Chand, S. 2010. Charge transport and microstructure in PFO: MEH-PPV polymer blend thin films. *Synthetic Metals* 160(15-16): 1740-1744.

Carter, S.A., Scott, J.C. & Brock, P.J. 1997. Enhanced luminance in polymer composite light emitting devices. *Applied Physics Letters* 71:1145.

Dow, J.D. & Redfield, D. 1970. Electroabsorption in semiconductors: The excitonic absorption edge. *Physical Review B* 1(8): 3358-3371.

Dutta, K. & De, S.K. 2006. Transport and optical properties of $SiO_2$–polypyrrole nanocomposites. *Solid State Communications* 140(3-4): 167-171.

Elliott, S.R. 1998. *The Physics and Chemistry of Solids*. London: J. Wiley.

Ginger, D.S. & Greenham, N.C. 1999. Charge separation in conjugated-polymer/nanocrystal blends. *Synthetic Metals* 101(1-3): 425-428.

Hagler, T.W., Pakbaz, K., Voss, K.F. & Heeger, A.J. 1991. Enhanced order and electronic delocalization in conjugated polymers oriented by gel processing in polyethylene. *Physical Review B* 44(16): 8652-8666.

Han, Z., Zhang, J., Yang, X., Zhu, H. & Cao, W. 2010. Synthesis and application in solar cell of poly(3-Octylthiophene)/titania nanotubes composite. *Organic Electronics* 11(8): 1449-1460.

Ho, P.K.H. & Friend, R.H. 2002. Π-electronic and electrical transport properties of conjugated polymer nanocomposites: Poly (P-Phenylenevinylene) with homogeneously dispersed silica nanoparticles. *The Journal of Chemical Physics* 116: 6782-6795.

Huang, Y., Qin, Y., Zhou, Y., Niu, H., Yu, Z-Z. & Dong, J-Y. 2010. Polypropylene/graphene oxide nanocomposites prepared by *in situ* Ziegler–Natta polymerization. *Chemistry of Materials* 22(13): 4096-4102.

Ibrahim, S., Ahmad, R. & Johan, M.R. 2012. Conductivity and optical studies of plasticized solid polymer electrolytes doped with carbon nanotube. *Journal of Luminescence* 132(1): 147-152.

Jafarzadeh, M., Rahman, I.A. & Sipaut, C.S. 2009. Synthesis of silica nanoparticles by modified sol–gel process: The effect of mixing modes of the reactants and drying techniques. *Journal of Sol-gel Science and Technology* 50(3): 328-336.

Kickelbick, G. 2003. Concepts for the incorporation of inorganic building blocks into organic polymers on a nanoscale. *Progress in Polymer Science* 28(1): 83-114.

Kim, K-S. & Park, S-J. 2012. Influence of N-doped $Tio_2$ on lithium ion conductivity of porous polymeric electrolyte membrane containing $LiClO_4$. *Solid State Ionics* 212: 18-25.

Liu, D., Teng, F., Xu, Z., Yang, S., Qian, L., He, Q., Wang, Y. & Xu, X. 2007. Enhanced brightness and efficiency in organic light-emitting diodes using $SiO_2$ as buffer layer and electron-blocking layer. *Journal of Luminescence* 122-123: 656-659.

Liu, J., Shi, Y. & Yang, Y. 2001. Improving the performance of polymer light-emitting diodes using polymer solid solutions. *Applied Physics Letters* 79: 578-580.

Peng, F., Lu, L., Sun, H., Wang, Y., Liu, J. & Jiang, Z. 2005. Hybrid organic-inorganic membrane: Solving the tradeoff between permeability and selectivity. *Chemistry of Materials* 17(26): 6790-6796.

Pichler, K., Halliday, D.A., Bradley, D.D.C., Burn, P.L., Friend, R.H. & Holmes, A.B. 1993. Optical spectroscopy of highly ordered poly (P-Phenylene Vinylene). *Journal of Physics: Condensed Matter* 5: 7155-7172.

Raja, V., Sarma, A.K. & Rao, V.V.R. 2003. Optical properties of pure and doped Pmma-CO-P4VPNO polymer films. *Materials Letters* 57(30): 4678-4683.

Rozenberg, B.A. & Tenne, R. 2008. Polymer-assisted fabrication of nanoparticles and nanocomposites. *Progress in Polymer Science* 33(1): 40-112.

Tommalieh, M.J. & Zihlif, A.M. 2010. Optical properties of polyimide/silica nanocomposite. *Physica B: Condensed Matter* 405(23): 4750-4754.

Uragami, T., Matsugi, H. & Miyata, T. 2005. Pervaporation characteristics of organic-inorganic hybrid membranes composed of poly (vinyl alcohol-co-acrylic acid) and tetraethoxysilane for water/ethanol separation. *Macromolecules* 38(20): 8440-8446.

Urbach, F. 1953. The long-wavelength edge of photographic sensitivity and of the electronic absorption of solids. *Physical Review* 92: 1324.

Yang, S.H., Le Rendu, P., Nguyen, T.P. & Hsu, C.S. 2007. Fabrication of MEH-PPV/$SiO_2$. *Reviews on Advanced Materials Science* 15: 144-149.

Yang, S.H., Nguyen, T.P., Le Rendu, P. & Hsu, C.S. 2005. Optical and electrical investigations of poly (P-Phenylene Vinylene)/ silicon oxide and poly (P-Phenylene Vinylene)/titanium oxide nanocomposites. *Thin Solid Films* 471(1-2): 230-235.

Mohammad Hafizuddin Haji Jumali*, Bandar Ali Al-Asbahi & Chi Chin Yap
School of Applied Physics, Faculty of Science and Technology
Universiti Kebangsaan Malaysia
43600 UKM Bangi, Selangor, D.E.
Malaysia

Bandar Ali Al-Asbahi
Department of Physics, Faculty of Science
Sana'a University
Yemen

Muhamad Mat Salleh
Institute of Microengineering and Nanoelectronics (IMEN)
Universiti Kebangsaan Malaysia
43600 UKM Bangi, Selangor, D.E.
Malaysia

Mohamad Saleh AlSalhi
Department of Physics and Astronomy
Laser Group, College of Science
King Saud University
Saudi Arabia

*Corresponding author; email: hafizhj@ukm.my

Received: 11 June 2012
Accepted: 2 February 2013